UCI-TR-2012-16, FERMILAB-PUB-12-560-PPD, LA-UR-12-25423

Compatibility of θ_{13} and the Type I Seesaw Model with A_4 Symmetry

Mu-Chun Chen,[1] Jinrui Huang,[1,2] Jon-Michael O'Bryan,[1] Alexander M. Wijangco,[1] and Felix Yu[3]

[1]*Department of Physics and Astronomy,*
University of California, Irvine, CA 92697, USA

[2]*Theoretical Division, T-2, MS B285,*
Los Alamos National Laboratory, Los Alamos, NM 87545, USA

[3]*Theoretical Physics Department, Fermi National Accelerator Laboratory,*
P.O. Box 500, Batavia, IL 60510, USA

(Dated: January 10, 2013)

arXiv:1210.6982v2 [hep-ph] 8 Jan 2013

Abstract

We derive formulae for neutrino masses and mixing angles in a type I seesaw framework with an underlying A_4 flavor symmetry. In particular, the Majorana neutrino mass matrix includes contributions from an A_4 triplet, 1, $1'$, and $1''$ flavon fields. Using these formulae, we constrain the general A_4 parameter space using the updated global fits on neutrino mixing angles and mass squared differences, including results from the Daya Bay and RENO experiments, and we find predictive relations among the mixing parameters for certain choices of the triplet vacuum expectation value. In the normal hierarchy case, sizable deviation from maximal atmospheric mixing is predicted, and such deviation is strongly correlated with the value of θ_{13} in the range of $\sim (8-10)^\circ$. On the other hand, such deviation is negligible and insensitive to θ_{13} in the inverted mass hierarchy case. We also show expectations for the Dirac CP phase resulting from the parameter scan. Future refined measurements of neutrino mixing angles will test these predicted correlations and potentially show evidence for particular triplet vev patterns.

Operated by Fermi Research Alliance, LLC under Contract No. De-AC02-07CH11359 with the United States Department of Energy.

I. INTRODUCTION

With the independent discoveries of a nonzero θ_{13} from the Daya Bay [1] and RENO [2] collaborations, and the supporting hints from the T2K [3], MINOS [4], and Double Chooz [5] experiments, we now possess the first complete experimental picture of the Pontecorvo-Maki-Nakagawa-Sakata (PMNS) mixing matrix. Following a recent global analysis of neutrino oscillation parameters from Ref. [6] (see also [7–9] and [10–12]), we can summarize the experimental status to date as

$$\sin^2\theta_{12} = 0.320^{+0.015}_{-0.017} , \tag{1}$$

$$\sin^2\theta_{23} = \begin{cases} 0.49^{+0.08}_{-0.05} & \text{(Normal)} \\ 0.53^{+0.05}_{-0.07} & \text{(Inverted)} \end{cases} , \tag{2}$$

$$\sin^2\theta_{13} = \begin{cases} 0.026^{+0.003}_{-0.004} & \text{(Normal)} \\ 0.027^{+0.003}_{-0.004} & \text{(Inverted)} \end{cases} , \tag{3}$$

$$\Delta m^2_{21} = 7.62 \pm 0.19 \times 10^{-5}\ \text{eV}^2 , \tag{4}$$

$$\Delta m^2_{31} = \begin{cases} 2.53^{+0.08}_{-0.10} \times 10^{-3}\ \text{eV}^2 & \text{(Normal)} \\ -(2.40^{+0.10}_{-0.07}) \times 10^{-3}\ \text{eV}^2 & \text{(Inverted)} \end{cases} . \tag{5}$$

Before the $\theta_{13} \neq 0$ discovery, the PMNS matrix was consistent with the tribimaximal (TBM) mixing pattern [13], which can be written as

$$U_{TBM} = \begin{pmatrix} \frac{2}{\sqrt{6}} & \frac{1}{\sqrt{3}} & 0 \\ -\frac{1}{\sqrt{6}} & \frac{1}{\sqrt{3}} & \frac{1}{\sqrt{2}} \\ \frac{1}{\sqrt{6}} & -\frac{1}{\sqrt{3}} & \frac{1}{\sqrt{2}} \end{pmatrix} , \tag{6}$$

where we have adopted the same phase convention as the PDG [14] for placement of the minus signs. The TBM mixing pattern gives the solar mixing angle corresponding to $\sin^2\theta_{12} = 1/3$, the atmospheric mixing angle $\sin^2\theta_{23} = 1/2$, and reactor mixing angle $\sin^2\theta_{13} = 0$. Neutrino mass matrices that give rise to TBM mixing have distinct invariants that can be traced to discrete symmetries such as the Klein $Z_2 \times Z_2$ group or the symmetry group S_4 [15–18] (see also, [19]). On the other hand, by introducing dynamical (flavon) fields, the TBM mixing pattern can arise from a smaller underlying finite group, the tetrahedral group, A_4. To be compatible with grand unification, a successful generation of appropriate lepton and quark masses and mixing angles can be achieved by considering T', the double covering group of A_4. In an $SU(5)$ grand unified model [20], the T' group also affords a novel origin of CP violation from complex Clebsch-Gordan coefficients [21], while in a Randall-Sundrum model [22, 23], the T' flavor symmetry is simultaneously used to

forbid tree-level flavor-changing neutral currents (FCNCs). For reviews of the status of A_4 and S_4 models, the tribimaximal and bimaximal paradigm, see [24–26]. For early work in mixing and GUT theories, see [27].

The literature on the interrelation between TBM neutrino mixing matrices and finite group flavor symmetries is vast. With discovery of a nonzero θ_{13} from Daya Bay and RENO, however, the TBM prediction for a vanishing reactor angle is ruled out, calling into question the entire TBM paradigm. We emphasize, however, that the underlying flavor symmetries that naturally give rise to TBM mixing are nevertheless viable options for explaining the updated PMNS mixing pattern. In particular, we demonstrate that A_4, when we include flavons that are not included in the usual TBM analysis, can readily accommodate a large value of θ_{13} and retain predictivity for δ, the PMNS CP-violating Dirac phase.

Work before the Daya Bay and RENO results that focused on finite group symmetries and generating nonzero θ_{13} includes [28], which studied corrections to TBM from higher dimensional operators and [29], which discussed renormalization group (RG) equations in see-saw models. More recent work looking to use higher dimensional operators to generate violations of the TBM scheme or neutrino phenomenology include [30, 31]. The authors of [32] conclude higher dimension operators and RG effects are equally important for leptogenesis. In [33], it was found that the size of corrections to neutrino mixing sum rules coming from renormalization group running are small. Correspondingly, in [34], it was shown that a large θ_{13} value cannot be generated through running if θ_{13} starts at 0. In [35], NLO and NNLO expressions were given for neutrino mixing angles in hierarchal mass scenarios with sequential dominance.

Nevertheless, we note that it is possible, with the so-called Hilbert basis method [36], to construct supersymmetric models where these higher dimensional operators in the holomorphic superpotential vanish. On the other hand, certain flavon-induced corrections in the non-holomorphic Kähler potential [37] cannot be forbidden by *any* conventional symmetries. Hence, even in the original A_4 models where θ_{13} vanishes at leading order, once these Kähler corrections are properly taken into account, a sizable θ_{13} can be attained that is compatible with the current experimental value [38].

Much of the recent literature has focused solely on accommodating non-zero θ_{13} with low-energy perturbations to the TBM matrix and ignore or only briefly discuss the possible underlying UV physics responsible for these deviations. In this vein, one popular parametrization was introduced in [39], which introduced deviations from TBM values using s, a, and r for the solar, atmospheric, and reactor mixing angles, respectively. Further work along this line, such as parameter scans in

this space of deviations, include [40–48] and also [49–52], which used a similar approach but an equivalent set of parameters. One drawback of such approaches is that complete UV flavor models generally predict additional flavor violating effects, which are not captured in these low-energy deviation studies [53]. Separately, TBM and BM mixing scenarios were studied for the case of nearly degenerate neutrino masses where loop corrections provide large effects in mixing angles [54]. Loop corrections to the Type I seesaw Majorana neutrino mass matrix leading to nonzero θ_{13} were also studied in [55]. Studies of generating nonzero θ_{13} from breaking μ-τ symmetry include [56–58].

In this work, we adopt a top-down approach where we will constrain the UV parameter space by the low energy neutrino observables. While other A_4 studies may have looked at the additional effects from $1'$ and $1''$ flavons contributing to the Majorana neutrino mass matrix, including [59–65], they have generally considered the pattern of the vacuum expectation value (VEV) of the triplet flavon to be $\propto (1,1,1)^T$. Some earlier work has separately considered other forms of the triplet flavon, such as [66]. In addition, recent literature has focused on small perturbations from the $(1,1,1)^T$ triplet flavon structure as a mechanism for generating a nonzero θ_{13} [59, 67–69], where this small perturbation may arise from a vacuum misalignment correction.

In contrast, our work considers the full parameter space of A_4 flavons contributing to the Majorana mass matrix in the Type I seesaw. Thus we consider triplet flavon vevs that are markedly different from the usual TBM $(1,1,1)^T$ form simultaneously with the presence of $1'$ and $1''$ flavons. By looking at a completely general admixture of possibly flavon vevs, we can definitively constrain the entire A_4 parameter space in this Type I seesaw model. We remark that for the charged lepton masses and the Dirac neutrino masses, we introduce the minimal field content to generate their mass matrices and only introduce the full flavon field content for the RH neutrino masses. Moreover, even though we consider a larger A_4 parameter space than the earlier literature, we still retain predictivity, especially when the triplet flavon vev pattern preserves a subgroup of A_4.

Here we concentrate on the group A_4, which is the smallest group that contains a triplet representation. Other groups that have been utilized include $O(2)$ and $SO(2)$ symmetry [70], $\Delta(3n^2)$ and $\Delta(6n^2)$ [71, 72], Δ_{96} [73, 74], Q_6 with three sterile neutrinos [75], and product groups of modular Z_n finite groups in various permutations [76–85]. Other studies have focused on permutation symmetry S_3 and S_4 models [86–92]. Other mixing scenarios beyond TBM and related patterns include democratic mixing, which has been studied in [43, 54, 93], tetra-maximal mixing [94], and anarchic mixing [95–98].

The paper is organized as follows. In Sec. II, we briefly review the A_4 finite group symmetry and our type-I seesaw model implementation. In Sec. III, we present the results of our parameter

	H	L	N	e_R	μ_R	τ_R	ϕ_E	ϕ_N	η	χ	ψ
A_4	**1**	**3**	**3**	**1**	**1″**	**1′**	**3**	**3**	**1**	**1′**	**1″**
Z_2	**1**	**1**	**1**	**-1**	**-1**	**-1**	**-1**	**1**	**1**	**1**	**1**

TABLE I: The A_4 and Z_2 charge assignments of the Standard Model fields and A_4 flavons.

scan of the A_4 flavor vev space. We conclude in Sec. IV. An intermediate step of our calculation is presented in Appendix A.

II. THE A_4 MODEL

We construct a Type I seesaw model based on an A_4 flavor symmetry. We include three right-handed neutrinos N_i, which are Standard Model gauge singlets. These neutrinos transform as a triplet **3** under A_4. We also assign the lepton $SU(2)$ doublet $L \sim \mathbf{3}$, charged lepton $SU(2)$ singlets $e_R \sim \mathbf{1}$, $\mu_R \sim \mathbf{1}''$, $\tau_R \sim \mathbf{1}'$. To separate the charged lepton coupling scalars from the neutrino coupling scalars, we impose a Z_2 symmetry. These representations are summarized in Table I.

The Lagrangian for the leptons is

$$\begin{aligned}\mathcal{L} \supset & \left(H\bar{L}\left(\lambda_e e_R + \lambda_\mu \mu_R + \lambda_\tau \tau_R\right)\left(\frac{\phi_E}{\Lambda}\right) + \lambda_N \tilde{H}\bar{L}N + \text{ h.c.}\right) \\ & + \Lambda_{RR} N^T N \left(\frac{c_N\phi_N + c_\eta \eta + c_\chi \chi + c_\psi \psi}{\Lambda}\right) + c.c. \ ,\end{aligned} \tag{7}$$

where $\phi_E \sim \mathbf{3}$, $\phi_N \sim \mathbf{3}$, $\eta \sim \mathbf{1}$, $\chi \sim \mathbf{1}'$, and $\psi \sim \mathbf{1}''$ are scalar fields which acquire vevs and break the A_4 symmetry at the scale Λ, and the couplings c_N, c_η, c_χ, and c_ψ are complex. However, we absorb all phases (including Majorana phases) into c_N and thus c_N is indexed to be non-universal. We will not specify here the scalar potential to give the ϕ_E, ϕ_N, η, χ, and ψ fields vevs, but instead we leave a study of the potential construction and vacuum alignment questions for future work. The Lagrangian includes the familiar Dirac masses for the charged leptons, new Dirac masses for the neutrinos, and a general A_4–invariant Majorana mass matrix which includes all possible A_4 contractions. Thus, in contrast with early, pre-Daya Bay and RENO models that generated exact TBM mixing by including only the $\phi_N \sim (1,1,1)^T$ and η flavons, we include the χ and ψ flavons and allow ϕ_N vev to be less constrained: subcategories of our approach have also been considered previously [59–65].

The explicit form of the resulting mass matrices for the charged leptons and neutrinos is easily obtained from the A_4 invariants, which are reviewed, for example, in Ref. [24]. We assume ϕ_E acquires a vev $\langle\phi_E\rangle = \Lambda(1,0,0)^T$, and thus after electroweak symmetry breaking whereby the

Higgs acquires a vev v_h, the charged lepton mass matrix is

$$\bar{L}M_L e = \bar{L}v_h \begin{pmatrix} \lambda_e & 0 & 0 \\ 0 & \lambda_\mu & 0 \\ 0 & 0 & \lambda_\tau \end{pmatrix} e \ , \tag{8}$$

where $e = (e_R, \mu_R, \tau_R)$. The corresponding Dirac mass matrix for the neutrinos is simply governed by the A_4 contraction of L and N, giving

$$\lambda_N \tilde{H}\bar{L}N = \bar{L}M_{Dc}N = \bar{L} \begin{pmatrix} \lambda_N v_h & 0 & 0 \\ 0 & 0 & \lambda_N v_h \\ 0 & \lambda_N v_h & 0 \end{pmatrix} N \ . \tag{9}$$

For the Majorana mass matrix, we will be more general and allow ϕ_N to obtain a general vev pattern, $c_N\langle\phi_N\rangle = \Lambda(\phi_a, \phi_b, \phi_c)$. In addition, we let $c_\eta\langle\eta\rangle = \Lambda\eta$, and similarly for χ and ψ, such that the vev parameters η, χ, and ψ are dimensionless and have absorbed their respective Lagrangian couplings. We have the Majorana mass matrix

$$M_N N^T N = \Lambda_{RR} N^T N \begin{pmatrix} \frac{2}{3}\phi_a + \eta & -\frac{1}{3}\phi_c + \psi & -\frac{1}{3}\phi_b + \chi \\ -\frac{1}{3}\phi_c + \psi & \frac{2}{3}\phi_b + \chi & -\frac{1}{3}\phi_a + \eta \\ -\frac{1}{3}\phi_b + \chi & -\frac{1}{3}\phi_a + \eta & \frac{2}{3}\phi_c + \psi \end{pmatrix} \ . \tag{10}$$

It is worth noting that there is another term one could write, $m_{RR}N^T N$, which sets an additional mass scale m_{RR} which we will designate as Λ_{RR}. We absorb this term into the vev of η. Since N is a gauge singlet, there is no connection between the Higgs vev and the mass scale Λ_{RR}. In particular, if we set $\Lambda_{RR} \sim \mathcal{O}(\Lambda_{GUT}) \approx 10^{16}$ GeV, we exercise the seesaw mechanism to generate light neutrino masses. Moreover, we assume the A_4 breaking scale $\Lambda \sim 0.1\Lambda_{RR}$ to avoid tuning issues between the mass scale and the breaking scale. The block matrix for the neutrinos in the $(\nu_L, N)^T$ basis is

$$M_\nu = \begin{pmatrix} 0 & M_{Dc}^T \\ M_{Dc} & M_N \end{pmatrix} \ , \tag{11}$$

which generates the effective neutrino mass matrix

$$M_{\nu,\ \mathrm{eff}} = M_{Dc} M_N^{-1} M_{Dc}^T \ , \tag{12}$$

after the right-handed neutrinos have been integrated out.

Now, in exact analogy with the Cabibbo-Kobayashi-Maskawa (CKM) matrix, the PMNS matrix arises when we express the weak charged current interactions in the lepton mass basis. The PMNS

matrix is

$$V_{PMNS} = U_L U_\nu^\dagger \ , \tag{13}$$

where

$$M_L^{\rm diag} = U_L M_L U_L^\dagger \ , \quad M_\nu^{\rm diag} = U_\nu M_{\nu,\ {\rm eff}} U_\nu^\dagger \ , \tag{14}$$

but from Eq. (8), $U_L = \mathbf{1}_3$, and thus the PMNS matrix is identified with the neutrino diagonalization matrix $U_\nu^\dagger$. The three parameters λ_e, λ_μ, and λ_τ, which are each rescaled by $\langle\phi_E\rangle/\Lambda$, are in one-to-one correspondence with the three charged lepton masses and are hence fixed.

Having identified $V_{PMNS} \equiv U_\nu^\dagger$, we adopt the standard parametrization of the PMNS matrix given by

$$V_{PMNS} = \begin{pmatrix} 1 & 0 & 0 \\ 0 & c_{23} & s_{23} \\ 0 & -s_{23} & c_{23} \end{pmatrix} \begin{pmatrix} c_{13} & 0 & s_{13}e^{-i\delta} \\ 0 & 1 & 0 \\ -s_{13}e^{i\delta} & 0 & c_{13} \end{pmatrix} \begin{pmatrix} c_{12} & s_{12} & 0 \\ -s_{12} & c_{12} & 0 \\ 0 & 0 & 1 \end{pmatrix} \ {\rm diag}(1, e^{i\xi_1}, e^{i\xi_2}) \ , \tag{15}$$

where $c_{ij} = \cos\theta_{ij}$, $s_{ij} = \sin\theta_{ij}$, δ is the Dirac phase, ξ_1 and ξ_2 are the Majorana phases, with $0 \leq \theta_{ij} \leq \pi/2$, $0 \leq \delta$, $\xi_1, \xi_2 \leq 2\pi$.

We now have a solvable system of equations relating the neutrino masses, mixing angles, and phases with the flavon vevs. From Eq. (12), Eq. (14), and using $U_\nu^\dagger = V_{PMNS}$, we find the relation

$$M_{Dc} M_N^{-1} M_{Dc}^T = M_{\nu\ {\rm eff}} = U_\nu^\dagger M_\nu^{\rm diag} U_\nu = V_{PMNS} M_\nu^{\rm diag} V_{PMNS}^\dagger \ , \tag{16}$$

where M_N is given in Eq. (10). Solving for M_N^{-1} and inverting, we get

$$M_N = M_{Dc}^T V_{PMNS} (M_\nu^{\rm diag})^{-1} V_{PMNS}^\dagger M_{Dc} \ . \tag{17}$$

Entry by entry, we have a system of six equations that can be solved analytically, which gives exact relations between the A_4 parameter space and the physical masses and PMNS mixing angles. This is manifestly symmetric, which is most easily seen from Eq. (10). A similar result using the mass entries of the Majorana mass matrix instead of the triplet and one-dimensional flavon vevs was the starting point of [64]. Our approach, in contrast, directly shows the correlation between different UV triplet flavons and low energy neutrino observables.

Naively, we have a six-dimensional UV parameter space, given by the three components of the ϕ_N triplet flavon and each of the one-dimensional flavons. The flavon breaking scale Λ and the Majorana mass scale are unobservable and can be absorbed into the six flavon vev components.

Subgroup	vev alignment
Z_2	$(1,0,0)$, $(0,1,0)$, $(0,0,1)$
Z_3	$(-1,1,1)$, $(1,1,-1)$, $(1,-1,1)$, $(1,1,1)$
breaking	$(0,1,1)$, $(1,0,1)$, $(1,1,0)$, $(0,1,-1)$, $(2,1,1)$, $(1,1,2)$, $(1,2,1)$, $(1,-2,1)$, $(1,1,-2)$, $(-2,1,1)$

TABLE II: Listed vev alignments for ϕ that preserve a Z_2 or Z_3 subgroup of A_4.

Now, although the triplet's vevs can be independent degrees of freedom, certain breaking alignments in flavon space preserve the Z_2 or Z_3 subgroups of A_4 and thus reduce the number of UV parameters. We will thus categorize our results according to subgroup preserving and subgroup breaking triplet vev patterns, which are listed in Table II. Subgroup preserving vev patterns thus effectively have a four-dimensional parameter space, while subgroup breaking vev patterns have a six-dimensional space.

In general, there are nine physical parameters which give rise to eight physical predictions: three mixing angles, three masses, and one Dirac CP phase, as well as two Majorana phases that combine to dictate the rate of neutrinoless double β decay. We will not discuss $0\nu2\beta$ further in this paper, and instead focus on the three angles, three masses, and the Dirac CP phase. We can thus see both our subgroup preserving and subgroup breaking categories are predictive: the four parameters in the subgroup preserving category, for instance, are over-constrained by the existing neutrino measurements, and the existence of a nontrivial solution reflects the suitability of the A_4 finite group as a possible flavor symmetry of the lepton sector. In addition, for both categories, the yet-to-be-discovered Dirac CP phase is predicted from our parameter scan, which we detail in the next section.

A. Breaking Bimaximality, Analytic Results

We present an analytic understanding of breaking bimaximality (*i.e.* deviations of θ_{23} from $45°$) in our general Type I seesaw A_4 construction. First, we calculate the effective neutrino mass matrix, and then analyze to the extent a $\theta_{23} = 45°$ rotation diagonalizes this matrix. Starting with Eq. (9), we write

$$M_{Dc} = M_{Dc}^T = \lambda_N v_h \begin{pmatrix} 1 & 0 & 0 \\ 0 & 0 & 1 \\ 0 & 1 & 0 \end{pmatrix} , \tag{18}$$

and we can recognize that $M_{Dc}^{-1} = \frac{1}{\lambda_N^2 v_h^2} M_{Dc}$. Next, since U_ν is the diagonalization matrix of $M_{\nu,\,\mathrm{eff}}$, as established in Eq. (14), U_ν is also the diagonalization matrix of $M_{\nu,\,\mathrm{eff}}^{-1}$, since

$$(M_\nu^{\mathrm{diag}})^{-1} = (U_\nu M_{\nu,\,\mathrm{eff}} U_\nu^\dagger)^{-1} = (U_\nu^\dagger)^{-1}(M_{\nu,\,\mathrm{eff}})^{-1}(U_\nu)^{-1} = U_\nu (M_{\nu,\,\mathrm{eff}})^{-1} U_\nu^\dagger \ . \tag{19}$$

Thus, the seesaw mass matrix in Eq. (12) can be inverted to give

$$M_{\nu,\,\mathrm{eff}}^{-1} = \frac{1}{\lambda_N^4 v_h^4} M_{Dc} M_N M_{Dc}^T \ . \tag{20}$$

Recall that because our charged lepton mass matrix in Eq. (8) is diagonal, we have the identity $V_{PMNS} = U_\nu^\dagger$, so the diagonalization matrix of $M_{\nu,\,\mathrm{eff}}$, and by extension, $M_{\nu,\,\mathrm{eff}}^{-1}$ is the PMNS matrix.

Recall that the PMNS matrix is composed of three Jacobi rotation angles, ordered as a θ_{23} rotation, a θ_{13} rotation, and then a θ_{12} rotation, and the phase rotations, as we can see from Eq. (15). Also, recall that a Jacobi rotation operates on a 2×2 block of the matrix, such as

$$\begin{pmatrix} a & b \\ b & c \end{pmatrix} \ , \tag{21}$$

where the rotation angle is defined as

$$\tan 2\theta = \frac{2b}{c-a} \ . \tag{22}$$

In particular, for fixed c and a, the sign of b determines the sign of θ. Moreover, we know that a rotation matrix for a single angle $\alpha + \beta$ can be decomposed into first rotating by α and then by β. (This, of course, does not commute with rotations about other axes.) Hence, we can rotate $M_{\nu,\,\mathrm{eff}}^{-1}$ by $\theta_{23} = 45^\circ$ and then understand deviations from bimaximality by testing the remaining presence of off-diagonal entries in the (3, 2) and (2, 3) entries of the effective neutrino mass matrix.

From Eq. (9) and Eq. (10), the RHS of Eq. (20) is

$$M_{\nu,\,\mathrm{eff}}^{-1} = \frac{1}{\lambda_N^2 v_h^2} \begin{pmatrix} \frac{2}{3}\phi_a + \eta & -\frac{1}{3}\phi_b + \chi & -\frac{1}{3}\phi_c + \psi \\ -\frac{1}{3}\phi_b + \chi & \frac{2}{3}\phi_c + \psi & -\frac{1}{3}\phi_a + \eta \\ -\frac{1}{3}\phi_c + \psi & -\frac{1}{3}\phi_a + \eta & \frac{2}{3}\phi_b + \chi \end{pmatrix} \ , \tag{23}$$

which as a trivial check, is still symmetric. After we perform the $\theta_{23} = 45^\circ$ bimaximal rotation, we have

$$R_{BM}^T M_{\nu,\,\mathrm{eff}}^{-1} R_{BM} = \begin{pmatrix} \frac{2}{3}\phi_a + \eta & \frac{1}{3\sqrt{2}}(-\phi_b + \phi_c) + \frac{1}{\sqrt{2}}(\chi - \psi) & \frac{-1}{3\sqrt{2}}(\phi_b + \phi_c) + \frac{1}{\sqrt{2}}(\chi + \psi) \\ \frac{1}{3\sqrt{2}}(-\phi_b + \phi_c) + \frac{1}{\sqrt{2}}(\chi - \psi) & \frac{1}{3}(\phi_a + \phi_b + \phi_c) - \eta + \frac{1}{2}\chi + \frac{1}{2}\psi & \frac{1}{3}(-\phi_b + \phi_c) - \frac{1}{2}\chi + \frac{1}{2}\psi \\ \frac{-1}{3\sqrt{2}}(\phi_b + \phi_c) + \frac{1}{\sqrt{2}}(\chi + \psi) & \frac{1}{3}(-\phi_b + \phi_c) - \frac{1}{2}\chi + \frac{1}{2}\psi & \frac{1}{3}(-\phi_a + \phi_b + \phi_c) + \eta + \frac{1}{2}\chi + \frac{1}{2}\psi \end{pmatrix} . \tag{24}$$

So, if $\frac{1}{3}(-\phi_b + \phi_c) - \frac{1}{2}\chi + \frac{1}{2}\psi \neq 0$, then the $\theta_{23} = 45^\circ$ bimaximal rotation was insufficient to eliminate the (3, 2) and (2, 3) entries and an additional θ_{23} rotation is needed. (In addition, if the (2, 2) and (3, 3) entries are identical, then $\theta_{23} = 45^\circ$ is guaranteed.) Moreover, we see that the transformation $\phi_b \leftrightarrow \phi_c$ and $\chi \leftrightarrow \psi$ changes the sign of the (3, 2) and (2, 3) entries while leaving the (2, 2) and (3, 3) entries fixed. Hence, we can see that any viable solution characterized by a triplet vev of (ϕ_a, ϕ_b, ϕ_c) and a particular set of η, χ, and ψ can be transmuted to a different solution characterized by (ϕ_a, ϕ_c, ϕ_b) and η, ψ, and χ with an opposite sign of the deviation from $\theta_{23} = 45^\circ$.

III. PARAMETER SCAN RESULTS FOR SUBGROUP PRESERVING AND SUBGROUP BREAKING TRIPLET FLAVON VEVS

Since current neutrino experiments do not have sensitivity to individual neutrino masses, we constrain the low energy neutrino observables by fitting to three mixing angles, two Δm^2, and the cosmological constraint on the sum of absolute neutrino masses. Clearly, the remaining parameter space for δ is the predictive relation from our parameter scan. (As stated before, we do not discuss the sensitivity to the Majorana phases from neutrino-less double β decay experiments.) We first take the system of equations in Eq. (17) and solve for the A_4 breaking vevs in terms of the neutrino observables. These solutions are presented in Appendix A. Since we want to work from the top-down, however, we partially invert the system to solve for the neutrino masses and the A_4 singlet vevs in terms of the A_4 triplet vev and the neutrino mixing angles and the CP phase. We obtain

$$m_i = \frac{v_h^2}{\Lambda_{RR}}(a^i b^j c^k \epsilon_{ijk})(\phi_a b^k c^j \epsilon_{ijk} + \phi_b a^j c^k \epsilon_{ijk} + \phi_c a^k b^j \epsilon_{ijk})^{-1} \ , \tag{25}$$

where m_1, m_2, m_3 are the three light neutrino masses, i, j, $k = 1, 2, 3$, and ϵ_{ijk} is the Levi-Civita tensor. The three-component vectors $\vec{a}$, $\vec{b}$, $\vec{c}$ are found in Table III.

This partial inversion is advantageous because, using the measured mixing angles, we can test individual A_4 triplet vevs and determine the fit to the correct mass squared differences and the cosmological constraint. We reparametrize the mass squared difference constraints into a ratio Δ_{21}/Δ_{31}, where $\Delta_{ij} \equiv m_i^2 - m_j^2$ and use the dimensionless ratio to constrain the dimensionless vevs in Eq. (25). The mass scale v_h^2/Λ_{RR} is then fixed by matching either of the measured mass squared differences.

In line with our top-down approach and intuition about the A_4 finite group, we attempt to preserve many of the symmetries present in the case of TBM mixing. Yet, simply relaxing $\sin^2\theta_{13} = 0$

a_1	$\left[c_{12}^2 c_{13}^2 - \left(s_{12}s_{23} - e^{-i\delta}c_{12}c_{23}s_{13}\right)\left(-c_{23}s_{12} - e^{i\delta}c_{12}s_{13}s_{23}\right)\right]$
a_2	$e^{-i2\xi_1}\left[c_{13}^2 s_{12}^2 + \left(c_{12}s_{23} + e^{-i\delta}c_{23}s_{12}s_{13}\right)\left(c_{12}c_{23} - e^{i\delta}s_{12}s_{13}s_{23}\right)\right]$
a_3	$e^{-i2\xi_2}(s_{13}^2 - c_{13}^2 c_{23}s_{23})$
b_1	$\left[\left(s_{12}s_{23} - e^{-i\delta}c_{12}c_{23}s_{13}\right)\left(s_{12}s_{23} - e^{i\delta}c_{12}c_{23}s_{13}\right) + c_{12}c_{13}\left(c_{23}s_{12} + e^{-i\delta}c_{12}s_{13}s_{23}\right)\right]$
b_2	$e^{-i2\xi_1}\left[\left(c_{12}s_{23} + e^{-i\delta}c_{23}s_{12}s_{13}\right)\left(c_{12}s_{23} + e^{i\delta}c_{23}s_{12}s_{13}\right) - c_{13}s_{12}\left(c_{12}c_{23} - e^{-i\delta}s_{12}s_{13}s_{23}\right)\right]$
b_3	$e^{-i2\xi_2}(c_{13}^2 c_{23}^2 - e^{-i\delta}c_{13}s_{13}s_{23})$
c_1	$\left[c_{12}c_{13}\left(-s_{12}s_{23} + e^{-i\delta}c_{12}c_{23}s_{13}\right) + \left(c_{23}s_{12} + e^{i\delta}c_{12}s_{13}s_{23}\right)\left(c_{23}s_{12} + e^{-i\delta}c_{12}s_{13}s_{23}\right)\right]$
c_2	$e^{-i2\xi_1}\left[c_{13}s_{12}\left(c_{12}s_{23} + e^{-i\delta}c_{23}s_{12}s_{13}\right) + \left(c_{12}c_{23} - e^{i\delta}s_{12}s_{13}s_{23}\right)\left(c_{12}c_{23} - e^{-i\delta}s_{12}s_{13}s_{23}\right)\right]$
c_3	$e^{-i2\xi_2}(c_{13}^2 s_{23}^2 - e^{-i\delta}c_{13}c_{23}s_{13})$

TABLE III: The explicit components of $\vec{a}$, $\vec{b}$, $\vec{c}$ as function of mixing angles and the triplet ϕ.

while simultaneously keeping the other TBM mixing angle relations did not lead to viable solutions without perturbing the triplet vev alignment. We therefore choose to relax the bimaximal relation $\sin^2\theta_{23} = \frac{1}{2}$ and maintain the trimaximal relation $\sin^2\theta_{12} = \frac{1}{3}$. In this way, we can understand a larger region of A_4 parameter space since the experimental bounds on θ_{12} are tighter than those on θ_{23}. Given this fixed θ_{12}, we then choose each of the Dirac and Majorana phases to be 0 or π for each triplet vev pattern.

However, this process itself is not entirely trivial, as not all choices are independent. Up to field re-phasing, there are four transformations about bimaximal mixing in which components of Eq. (25) transform antisymmetrically. Under the interchange of $\theta_{23} = 45^\circ + x \leftrightarrow \theta_{23} = 45^\circ - x$ and any of the four,

$$\begin{aligned}
\delta = 0, \xi_1 = 0, \xi_2 = 0 &\leftrightarrow \delta = \pi, \xi_1 = \pi, \xi_2 = \pi \\
\delta = 0, \xi_1 = \pi, \xi_2 = 0 &\leftrightarrow \delta = \pi, \xi_1 = \pi, \xi_2 = 0 \\
\delta = 0, \xi_1 = 0, \xi_2 = \pi &\leftrightarrow \delta = \pi, \xi_1 = 0, \xi_2 = \pi \\
\delta = 0, \xi_1 = \pi, \xi_2 = \pi &\leftrightarrow \delta = \pi, \xi_1 = 0, \xi_2 = 0 \ ,
\end{aligned} \tag{26}$$

we find

$$\begin{aligned}
\vec{a}\cdot(\vec{b}\times\vec{c}) &\leftrightarrow -\vec{a}\cdot(\vec{b}\times\vec{c}) \\
\vec{b}\times\vec{c} &\leftrightarrow \vec{c}\times\vec{b} \\
\vec{a}\times\vec{b} &\leftrightarrow \vec{a}\times\vec{c}\ .
\end{aligned} \tag{27}$$

It immediately follows that the existence of one solution implies there is a corresponding solution with different phases (and a possibly different triplet alignment) which is related under these

transformations. What remains to be specified are the angles θ_{23} and θ_{13}, which we scan over the 2σ θ_{23} range of [12] and over the 2σ θ_{13} experimental bounds from Daya Bay in Ref. [1] . We draw contours in this two-dimensional plane that satisfy the measured mass squared differences from [12] and we constrain the ratio of Δm^2 within 2σ uncertainties as dictated by the predicted neutrino hierarchy and set the individual neutrino mass scale using Λ_{RR}. From the existence of matter effects in solar neutrino oscillation, we know that $\Delta_{21} > 0$. So by enforcing this constrain upon the ratio there is a unique positive value and negative value for Δ_{21}/Δ_{31} that correspond to a normal or inverted neutrino mass hierarchy respectively. We then require the contours to satisfy the $\sum_i |m_{\nu_i}| < 0.81$ eV [99]. Because degenerate neutrino spectra lead to numerically unstable results, we discard possible solutions arising from degenerate neutrino spectra.

A. Numerical Results

These results are shown in the left panel of Fig. 1 for subgroup preserving triplet vev patterns from Table II that generate a normal hierarchy, while the right panel shows the subgroup preserving patterns that generate an inverted hierarchy. These figures clearly show the correlations between the deviation from the bimaximal θ_{23} and nonzero θ_{13}. Patterns that have such solutions are now uniquely determined and predict a very specific combination of masses and the CP phase. A notably absent alignment is the (1,1,1) breaking pattern, often associated with TBM mixing. We can understand this by considering Eq. (20) and asserting $\phi_a = \phi_b = \phi_c$. We find

$$f(\theta_{12}, \theta_{13}, \theta_{23})(m_2 - m_3) = 0 \ , \tag{28}$$

and so unless the function f is zero, the masses m_2 and m_3 are required to be degenerate and this vev is not a viable phenomenological alignment. Under exact TBM mixing, f is zero and the masses are free.

We also show the corresponding parameter scans for subgroup breaking triplet vev patterns that give normal hierarchies in the left panel of Fig. 2 and inverted hierarchies in the right panel. Although the parameter space is less predictive, we can nevertheless see that a normal hierarchy requires significant breaking of bimaximality, while an inverted hierarchy still allows for a bimaximal θ_{23} for some vev patterns.

For each successful triplet vev pattern and phase choice, we list the θ_{23} value and neutrino mass spectrum corresponding to the central value for θ_{13} from the Daya Bay collaboration [1] in Table IV.

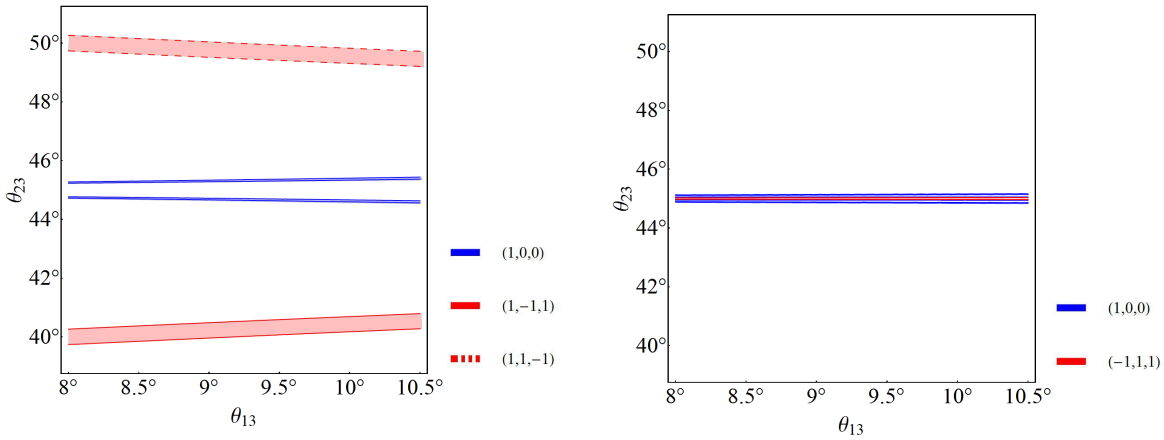

FIG. 1: Contour plots of Δ_{21}/Δ_{31} over the 2σ regions of θ_{23} and θ_{13} for subgroup preserving triplet vev patterns that generate (left panel) a normal hierarchy and (right panel) an inverted hierarchy. For normal hierarchies, we find the $(1,0,0)$ pattern stays close to the central angle of θ_{23}, while the the $(1,-1,1)$ and $(1,1,-1)$ patterns avoid the central value. The inverted hierarchy solutions, however, only deviate from the maximal angle of θ_{23} by values of order $\mathcal{O}(0.1°)$.

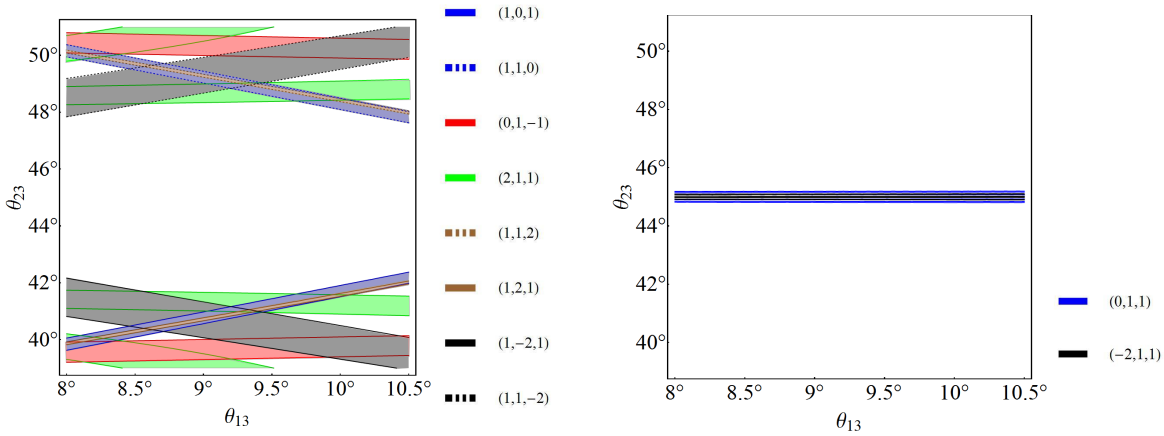

FIG. 2: Contour plots of Δ_{21}/Δ_{31} over the 2σ regions of θ_{23} and θ_{13} for subgroup breaking triplet vev patterns that generate (left panel) a normal hierarchy and (right panel) an inverted hierarchy. The normal hierarchy solutions characteristically avoid the central value of θ_{23}. Like the subgroup preserving vev patterns, here the inverted hierarchy solutions feature little deviations from the central value of θ_{23}

The vev alignments $(1,0,0)$ and the permutations of $(-1,1,1)$ comprising the first and second sets of solutions shown in Table IV are vevs preserving the Z_3 and Z_2 subgroups, respectively. The remaining vev alignments break A_4 completely. Each vev alignment can produce some deviation from $\theta_{23} = \pi/4$, and most notably, non-Z_3 preserving alignments can produce significant breaking of bimaximality where TBM cannot be approximate.

Generally, we find that inverted hierarchies feature deviations from θ_{23} from the TBM case of order $\mathcal{O}(0.1^\circ)$, while normal hierarchies favor deviations an order of magnitude larger. For a given choice of Dirac CP phase, we find that most breaking patterns are relatively insensitive to changes in θ_{13} with the current experimental bounds. We also highlight the fact that many simple A_4 triplet vev possibilities are excluded by the current experimental data. In particular, arbitrary triplet vev patterns in general will not generate the small hierarchy in experimental mass squared differences, and those that do are highly predictive about the extent of bimaximal breaking.

We can semi-analytically see why the normal hierarchy solutions deviate more strongly from bimaximality than the inverted hierarchy solutions. In general, for fixed θ_{12} and θ_{13}, we can consider a Taylor expansion of the neutrino masses around $z \equiv \theta_{23} - 45^\circ$,

$$\begin{aligned} m_1 &= x_1 + y_1 z + \dots \ , \\ m_2 &= x_2 + y_2 z + \dots \ , \\ m_3 &= x_3 + y_3 z + \dots \ , \end{aligned} \tag{29}$$

where $x_{1,2,3}$ and $y_{1,2,3}$ are the zeroth and first order coefficients. Using this expansion, we have

$$\Delta_{21} = m_2^2 - m_1^2 \approx x_2^2 - x_1^2 + 2(x_2 y_2 - x_1 y_1) z + \mathcal{O}(z^2) \ . \tag{30}$$

A complete expression of this mass squared difference for the central values of θ_{12} and θ_{13} and arbitrary triplet vev is not useful, but if we consider the special case of $\phi_b = \phi_c$, we generally find $x_1 = x_2$ and $y_1 = -y_2$, giving

$$\Delta_{21} \approx 4 x_2 y_2 z + \mathcal{O}(z^2) \ . \tag{31}$$

Furthermore, if we consider the behavior of the expansion coefficients x_1 and y_1 for normal hierarchy solutions versus related inverted hierarchy solutions, we find $x_1^{(N)} \approx x_1^{(I)}$ and $4 y_1^{(N)} \approx y_1^{(I)}$: from the Δ_{21} constraint, we see

$$z^{(N)} \approx 4 z^{(I)} \ , \tag{32}$$

which implies that the resulting deviation from bimaximality is much larger for normal hierarchies compared to inverted hierarchies. When exact expressions are used, the difference can be as big as an order of magnitude, as evident in the figures.

B. Dirac CP Phase Predictions

We now examine the predicted Dirac CP phase for various triplet vev patterns. Instead of fixing δ and scanning over θ_{23} and θ_{13} as before, we now set θ_{23} to the value preferred by the central

θ_{13} value of Daya Bay [1], as shown in Table IV, and scan this θ_{23} slice of the δ vs. θ_{13} plane. Contours that satisfy the correct mass squared differences are highlighted and shown in Fig. 3 for a few illustrative choices of vev patterns. Thus, for θ_{13} within the 2σ range of [1], the favored range of δ can be broad, as for the $(1, 1, -2)$ vev, or fairly narrow, as for the $(1, 1, -1)$, $(-1, 1, 1)$ and $(0, 1, 1)$ vevs. This figure shows that a measurement of δ and further refinement in narrowing the θ_{13} uncertainties can exclude or significantly favor a particular set of A_4 vev patterns. In addition, we see that shifts in the central value of θ_{13} will serve to disfavor particular vev patterns as well as better accommodate other vev patterns. Certainly, more data is needed to test these possibilities and the A_4 paradigm.

$(\phi_a^\nu, \phi_b^\nu, \phi_c^\nu)$	mass hierarchy	$(\xi_1, \xi_2, \delta, \theta_{23} - 45°)$	(m_1, m_2, m_3)
$(1, 0, 0)$	N	$(0, 0, \pi, -0.3°)$; $(\pi, \pi, 0, 0.3°)$	$(0.0447, 0.0455, -0.0667)$
$(1, 0, 0)$	I	$(\pi, 0, 0, -0.05°)$; $(\pi, 0, \pi, 0.05°)$	$(0.0618, -0.0624, 0.0370)$
$(1, 0, 0)$	I	$(0, 0, 0, -0.05°)$; $(\pi, \pi, \pi, 0.05°)$	$(0.0630, 0.0636, -0.0390)$
$(-1, 1, 1)$	I	$(0, 0, \pi, -0.03°)$; $(\pi, \pi, 0, 0.03°)$	$(-0.0496, -0.0504, 0.0035)$
$(1, -1, 1)$	N	$(0, 0, 0, -6.6°)$; $(\pi, \pi, \pi, 6.6°)$	$(0.0078, -0.0117, -0.0501)$
$(1, 1, -1)$	N	$(\pi, \pi, 0, -4.8°)$; $(0, 0, \pi, 4.8°)$	$(0.0032, -0.0093, 0.0496)$
$(0, 1, 1)$	I	$(\pi, \pi, \pi, -0.1°)$; $(0, 0, 0, 0.1°)$	$(0.0522, 0.0530, 0.0167)$
$(0, 1, 1)$	I	$(\pi, \pi, 0, -0.2°)$; $(0, 0, \pi, 0.2°)$	$(0.0522, 0.0530, 0.0167)$
$(2, 1, 1)$	N	$(0, 0, 0, -3.8°)$; $(\pi, \pi, \pi, 3.8°)$	$(0.0092, 0.0127, 0.0503)$
$(2, 1, 1)$	N	$(0, 0, \pi, -3.6°)$; $(\pi, \pi, 0, 3.6°)$	$(0.0210, 0.0227, 0.0538)$
$(-2, 1, 1)$	I	$(\pi, \pi, \pi, -0.02°)$; $(0, 0, 0, 0.02°)$	$(-0.0498, -0.0506, 0.0055)$
$(-2, 1, 1)$	I	$(0, 0, \pi, -0.1°)$; $(\pi, \pi, 0, 0.1°)$	$(-0.0523, -0.0530, 0.0168)$
$(0, 1, -1)$	N	$(\pi, \pi, 0, -5.4°)$; $(0, 0, \pi, 5.4°)$	$(0.0213, -0.0230, 0.0539)$
$(0, 1, -1)$	N	$(\pi, \pi, \pi, -7°)$; $(0, 0, 0, 7°)$	$(-0.0282, 0.0295, -0.0570)$
$(1, 0, 1); (1, 1, 0)$	N	$(\pi, 0, 0, -4.4°); (\pi, 0, \pi, 4.4°)$	$(0.0073, 0.0114, -0.0500)$
$(1, 2, 1); (1, 1, 2)$	N	$(0, \pi, \pi, -4.4°); (0, \pi, 0, 4.4°)$	$(0.0572, -0.0578, -0.0756)$
$(1, -2, 1); (1, 1, -2)$	N	$(\pi, \pi, 0, -4.2°); (0, 0, \pi, 4.2°)$	$(0.0074, -0.0114, -0.0500)$

TABLE IV: The collection of vev alignments considered in our parameter scan, resulting hierarchy, phases, deviation from bimaximality, and neutrino masses. The mass hierarchy column indicates whether the vev generates a normal (N) hierarchy or inverted (I) hierarchy. The last two columns indicate the required phases to obtain a valid mass hierarchy and the θ_{23} angle and neutrino masses corresponding to the central θ_{13} value from Daya Bay [1].

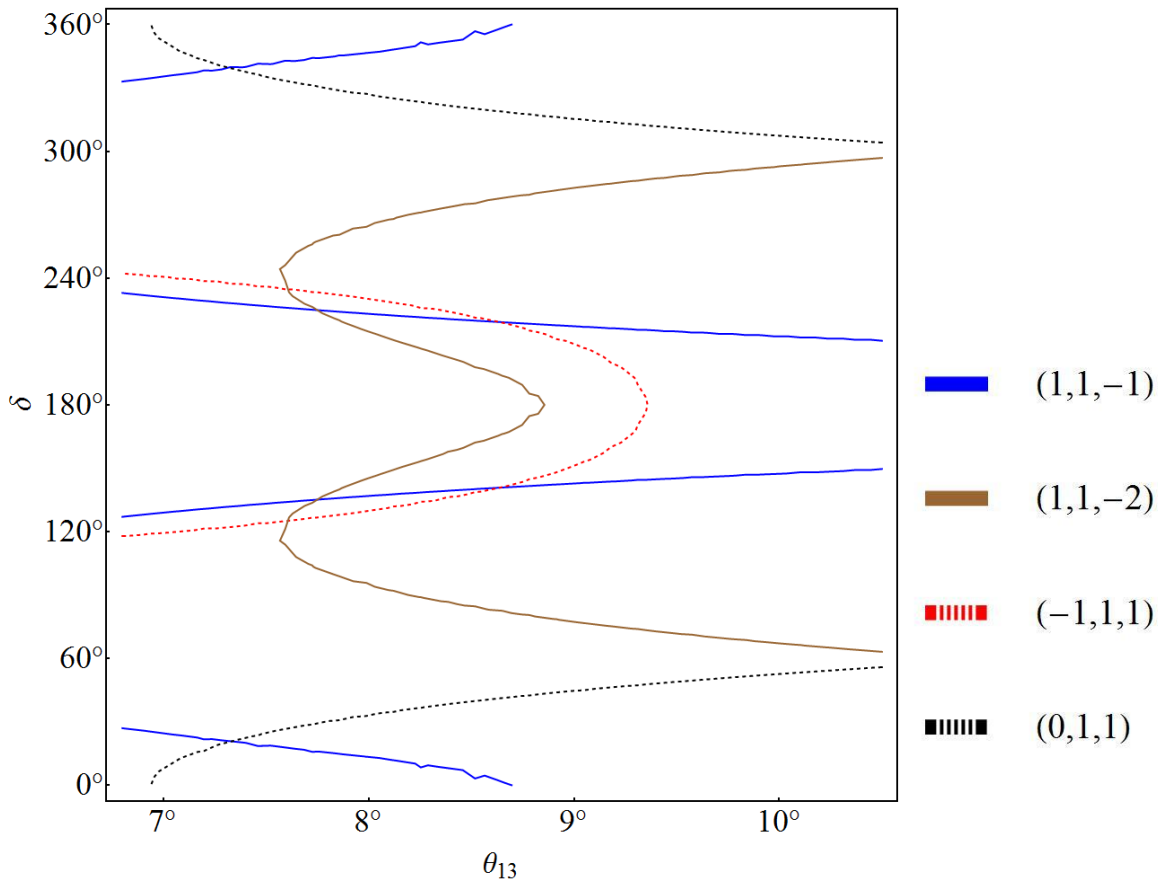

FIG. 3: Contours for various A_4 breaking patterns at their respective favored θ_{23} angle based on Table IV. The $(1,1,-1)$ and $(1,1,-2)$ patterns show the ratio contour for a normal mass hierarchy, while the $(-1,1,1)$ and $(0,1,1)$ show the ratio for an inverted mass hierarchy. The $(1,1,-1)$, $(-1,1,1)$, and $(0,1,1)$ vevs are moderately more predictive of δ than the $(-1,1,1)$ vev.

IV. CONCLUSIONS

In light of the results from the Daya Bay and RENO collaborations, we have developed a framework for understanding the constraints on the A_4 parameter space from low energy neutrino observables. For our parameter scan, we have assumed a Type I seesaw model with a minimal A_4 flavor structure governing the charged lepton masses and the Dirac neutrino masses, but the Majorana mass matrix has contributions from each of the possible $\mathbf{3}$, $\mathbf{1}$, $\mathbf{1}'$, and $\mathbf{1}''$ flavons, where the triplet vev pattern is initially unconstrained. We categorize the triplet vev according to Z_3 or Z_2 subgroup preserving patterns, which enhances the model predictivity: for these subgroup preserving patterns, four A_4 parameters are used to predict seven neutrino observables. Regarding the chosen vev patterns, we leave the question of scalar potentials or vacuum alignment for future work.

We have analyzed the A_4 parameter space in two distinct and intriguing slices. In the first case, we fix θ_{12} to be trimaximal and scan over the resulting θ_{23} vs. θ_{13} plane for various choices of Dirac and Majorana phases. The results show that vev patterns giving a normal neutrino mass hierarchy have moderately large breaking of bimaximality for θ_{23}, while inverted hierarchies generally retain bimaximality as a prediction. This indicates that a non-bimaximal θ_{23} measurement, such as the preliminary result $\sin^2(2\theta_{23}) = 0.94^{+0.04}_{-0.05}$ from MINOS [100] is favorably correlated with a normal hierarchy in our A_4 framework. We also analyzed the predictions for the Dirac CP phase δ for some illustrative choices of triplet vev pattern in the δ vs. θ_{13} plane. This analysis emphasizes the point that a future measurement of δ, decreased uncertainty in θ_{13}, and shifts in the central value of θ_{13} can strongly favor or exclude particular triplet vev patterns, highlighting the fact that future experimental results have significant power in discriminating possible A_4 flavon structures.

Acknowledgements

We would like to thank Michael Ratz for useful comments. M.-C.C. would like to thank the Technische Universität München (TUM), the Galileo Galilei Institute for Theoretical Physics (GGI), the Center for Theoretical Underground Physics and Related Areas (CETUP* 2012) in South Dakota, and the UC Gump Station on Moorea for their hospitality and for partial support during the completion of this work. M.-C.C. and FY acknowledge the hospitality of the Aspen Center for Physics, which is supported by the National Science Foundation Grant No. PHY-1066293. JH would like to thank the hospitality of the University of Washington where part of this work was completed. The work of M.-C.C. and JH is supported by the National Science Foundation under Grant No. PHY-0970173. JH is also supported by the DOE Office of Science and the LANL LDRD program. The work of JO'B and AW is supported by the NSF under Grant No. PHY-0970171. Fermilab is operated by Fermi Research Alliance, LLC under Contract No. De-AC02-07CH11359 with the United States Department of Energy.

Appendix A: General VEV Solutions of Flavon Fields

In Eq. (17), we have six equations that relate the A_4 flavons comprising the Majorana mass matrix to the low energy neutrino masses, mixing angles, and phases. We can solve this system to express the triplet flavon components, $(\phi_a, \phi_b, \phi_c)^T$, and the one-dimensional flavons, η, χ, and ψ,

in terms of the physical neutrino observables. This solution set is

$$\begin{aligned}
\langle\phi_a\rangle = F\Bigg(&\frac{1}{m_1}\left[c_{12}^2c_{13}^2-\left(s_{12}s_{23}-e^{-i\delta}c_{12}c_{23}s_{13}\right)\left(-c_{23}s_{12}-e^{i\delta}c_{12}s_{13}s_{23}\right)\right]\\
&+\frac{1}{m_2}e^{-i2\xi_1}\left[c_{13}^2s_{12}^2+\left(c_{12}s_{23}+e^{-i\delta}c_{23}s_{12}s_{13}\right)\left(c_{12}c_{23}-e^{i\delta}s_{12}s_{13}s_{23}\right)\right]\\
&+\frac{1}{m_3}e^{-i2\xi_2}(s_{13}^2-c_{13}^2c_{23}s_{23})\Bigg)\ , \qquad \text{(A1)}\\
\langle\phi_b\rangle = F\Bigg(&\frac{1}{m_1}\left[\left(s_{12}s_{23}-e^{-i\delta}c_{12}c_{23}s_{13}\right)\left(s_{12}s_{23}-e^{i\delta}c_{12}c_{23}s_{13}\right)+c_{12}c_{13}\left(c_{23}s_{12}+e^{-i\delta}c_{12}s_{13}s_{23}\right)\right]\\
&+\frac{1}{m_2}e^{-i2\xi_1}\left[\left(c_{12}s_{23}+e^{-i\delta}c_{23}s_{12}s_{13}\right)\left(c_{12}s_{23}+e^{i\delta}c_{23}s_{12}s_{13}\right)-c_{13}s_{12}\left(c_{12}c_{23}-e^{-i\delta}s_{12}s_{13}s_{23}\right)\right]\\
&+\frac{1}{m_3}e^{-i2\xi_2}(c_{13}^2c_{23}^2-e^{-i\delta}c_{13}s_{13}s_{23})\Bigg)\ , \qquad \text{(A2)}\\
\langle\phi_c\rangle = F\Bigg(&\frac{1}{m_1}\left[c_{12}c_{13}\left(-s_{12}s_{23}+e^{-i\delta}c_{12}c_{23}s_{13}\right)+\left(c_{23}s_{12}+e^{i\delta}c_{12}s_{13}s_{23}\right)\left(c_{23}s_{12}+e^{-i\delta}c_{12}s_{13}s_{23}\right)\right]\\
&+\frac{1}{m_2}e^{-i2\xi_1}\left[c_{13}s_{12}\left(c_{12}s_{23}+e^{-i\delta}c_{23}s_{12}s_{13}\right)+\left(c_{12}c_{23}-e^{i\delta}s_{12}s_{13}s_{23}\right)\left(c_{12}c_{23}-e^{-i\delta}s_{12}s_{13}s_{23}\right)\right]\\
&+\frac{1}{m_3}e^{-i2\xi_2}(c_{13}^2s_{23}^2-e^{-i\delta}c_{13}c_{23}s_{13})\Bigg)\ , \qquad \text{(A3)}\\
\langle\eta\rangle = \frac{F}{3}\Bigg(&\frac{1}{m_1}[c_{12}^2c_{13}^2+2(-s_{12}^2s_{23}c_{23}+c_{12}^2s_{13}^2s_{23}c_{23}+e^{-i\delta}c_{12}s_{12}s_{13}c_{23}^2-e^{i\delta}c_{12}s_{12}s_{13}s_{23}^2)]\\
&+\frac{1}{m_2}e^{-i2\xi_1}[c_{13}^2s_{12}^2-2c_{12}^2c_{23}s_{23}-2c_{12}s_{12}s_{13}(e^{-i\delta}c_{23}^2-e^{i\delta}s_{23}^2)+2s_{12}^2s_{13}^2s_{23}c_{23}]\\
&+\frac{1}{m_3}e^{-i2\xi_2}(s_{13}^2+2c_{13}^2c_{23}s_{23})\Bigg)\ , \qquad \text{(A4)}\\
\langle\psi\rangle = \frac{F}{3}\Bigg(&\frac{1}{m_1}[c_{23}^2s_{12}^2-c_{12}c_{23}s_{13}(2e^{-i\delta}c_{12}c_{13}-(e^{-i\delta}+e^{i\delta})s_{12}s_{23})+s_{23}(2c_{13}s_{12}c_{12}+c_{12}^2s_{13}^2s_{23})]\\
&+\frac{1}{m_2}e^{-i2\xi_1}[c_{12}^2c_{23}^2-(e^{-i\delta}+e^{i\delta})c_{12}c_{23}s_{12}s_{13}s_{23}-s_{12}(2e^{-i\delta}c_{23}s_{12}s_{13}c_{13}+s_{23}(2c_{12}c_{13}-s_{12}s_{13}^2s_{23}))]\\
&+\frac{1}{m_3}e^{-i2\xi_2}[c_{13}(2e^{-i\delta}c_{23}s_{13}+e^{i\delta}c_{13}s_{23})]\Bigg)\ , \qquad \text{(A5)}\\
\langle\chi\rangle = \frac{F}{3}\Bigg(&\frac{1}{m_1}[-2c_{13}c_{23}s_{12}c_{12}-(e^{-i\delta}+e^{i\delta})c_{12}c_{23}s_{12}s_{13}s_{23}+s_{12}^2s_{23}^2-c_{12}^2(-c_{23}^2s_{13}^2+2e^{-i\delta}s_{13}c_{13}s_{23})]\\
&+\frac{1}{m_2}e^{-i2\xi_1}[c_{12}^2s_{23}^2+s_{12}^2s_{13}(c_{23}^2s_{13}-2e^{-i\delta}c_{13}s_{23})+c_{12}c_{23}s_{12}(2c_{13}+(e^{-i\delta}+e^{i\delta})s_{13}s_{23})]\\
&+\frac{1}{m_3}e^{-i2\xi_2}[c_{13}(c_{13}c_{23}^2+2e^{-i\delta}s_{13}s_{23})]\Bigg)\ , \qquad \text{(A6)}
\end{aligned}$$

where $F = \dfrac{v_H^2\lambda_N^2}{\Lambda_{RR}}$. We invert Eq. (A1), Eq. (A2), and Eq. (A3) to solve for the neutrino masses in terms of the triplet vev components $(\phi_a, \phi_b, \phi_c)^T$. Then, we constrain the one-dimensional flavons and the neutrino masses by assuming a particular triplet vev pattern and scanning over the mixing angles and phases, applying the constraint on mass squared differences from [12] and

the cosmological bound on the sum of absolute neutrino masses from [14].

---

[1] F. An et al. (DAYA-BAY Collaboration), Phys.Rev.Lett. **108**, 171803 (2012), 5 figures. Version to appear in Phys. Rev. Lett, 1203.1669.

[2] J. Ahn et al. (RENO collaboration), Phys.Rev.Lett. **108**, 191802 (2012), 1204.0626.

[3] K. Abe et al. (T2K Collaboration), Phys.Rev.Lett. **107**, 041801 (2011), 1106.2822.

[4] P. Adamson et al. (MINOS Collaboration), Phys.Rev.Lett. **107**, 181802 (2011), 5 pages, 3 figures, 1108.0015.

[5] Y. Abe et al. (DOUBLE-CHOOZ Collaboration), Phys.Rev.Lett. **108**, 131801 (2012), 7 pages, 4 figures,, 1112.6353.

[6] M. Tortola, J. Valle, and D. Vanegas (2012), 1205.4018v1.

[7] G. Fogli, E. Lisi, A. Marrone, D. Montanino, A. Palazzo, et al. (2012), 1205.5254.

[8] S. Morisi and J. Valle (2012), 1206.6678.

[9] M. Gonzalez-Garcia, M. Maltoni, J. Salvado, and T. Schwetz (2012), 1209.3023.

[10] P. Machado, H. Minakata, H. Nunokawa, and R. Z. Funchal (2011), 1111.3330.

[11] T. Schwetz, M. Tortola, and J. Valle, New J.Phys. **13**, 109401 (2011), 1108.1376.

[12] T. Schwetz, M. Tortola, and J. Valle, New J.Phys. **13**, 063004 (2011), 1103.0734.

[13] P. Harrison, D. Perkins, and W. Scott, Phys.Lett. **B530**, 167 (2002), hep-ph/0202074.

[14] K. Nakamura et al. (Particle Data Group), J.Phys.G **G37**, 075021 (2010).

[15] C. Lam, Phys.Rev.Lett. **101**, 121602 (2008), 0804.2622.

[16] C. Lam, Phys.Rev. **D78**, 073015 (2008), 0809.1185.

[17] W. Grimus, L. Lavoura, and P. Ludl, J.Phys.G **G36**, 115007 (2009), 0906.2689.

[18] C. Lam (2009), 0907.2206.

[19] D. Hernandez and A. Y. Smirnov, Phys.Rev. **D86**, 053014 (2012), 1204.0445.

[20] M.-C. Chen and K. Mahanthappa, Phys.Lett. **B652**, 34 (2007), 0705.0714.

[21] M.-C. Chen and K. Mahanthappa, Phys.Lett. **B681**, 444 (2009), 0904.1721.

[22] M.-C. Chen, K. Mahanthappa, and F. Yu, Phys.Rev. **D81**, 036004 (2010), 0907.3963.

[23] M.-C. Chen, K. Mahanthappa, and F. Yu, AIP Conf.Proc. **1200**, 623 (2010), 0909.5472.

[24] G. Altarelli and F. Feruglio, Rev.Mod.Phys. **82**, 2701 (2010), 1002.0211.

[25] G. Altarelli, F. Feruglio, L. Merlo, and E. Stamou (2012), 1205.4670.

[26] G. Altarelli, F. Feruglio, and L. Merlo (2012), 1205.5133.

[27] P. Ramond, pp. 30–40 (2003), hep-ph/0401001.

[28] G. Altarelli and F. Feruglio, Nucl.Phys. **B720**, 64 (2005), hep-ph/0504165.

[29] S. Antusch, J. Kersten, M. Lindner, M. Ratz, and M. A. Schmidt, JHEP **0503**, 024 (2005), hep-ph/0501272.

[30] Y. Ahn, C. Kim, and S. Oh (2011), 1103.0657.

[31] Y. Ahn and S. K. Kang (2012), 1203.4185.

[32] I. K. Cooper, S. F. King, and C. Luhn, Nucl.Phys. **B859**, 159 (2012), 1110.5676.

[33] S. Boudjemaa and S. King, Phys.Rev. **D79**, 033001 (2009), 0808.2782.

[34] S. Luo and Z.-z. Xing (2012), 1203.3118.

[35] S. Antusch, S. Boudjemaa, and S. King, JHEP **1009**, 096 (2010), 27 pages, 2 figures, version to appear in JHEP, 1003.5498.

[36] R. Kappl, M. Ratz, and C. Staudt, JHEP **1110**, 027 (2011), 1108.2154.

[37] M. Leurer, Y. Nir, and N. Seiberg, Nucl.Phys. **B420**, 468 (1994), hep-ph/9310320.

[38] M.-C. Chen, M. Fallbacher, M. Ratz, and C. Staudt (2012), 1208.2947.

[39] S. King, Phys.Lett. **B659**, 244 (2008), 0710.0530.

[40] S. King, Phys.Lett. **B675**, 347 (2009), 0903.3199.

[41] Y. Ahn, H.-Y. Cheng, and S. Oh, Phys.Rev. **D84**, 113007 (2011), 20 pages and 8 figures, Accepted in Phys.Review D, 1107.4549.

[42] T. Araki, Phys.Rev. **D84**, 037301 (2011), 1106.5211.

[43] W. Chao and Y.-j. Zheng (2011), 1107.0738.

[44] Y.-j. Zheng and B.-Q. Ma, Eur.Phys.J.Plus **127**, 7 (2012), 1106.4040.

[45] B. Grinstein and M. Trott (2012), 1203.4410.

[46] X.-G. He and A. Zee, Phys.Rev. **D84**, 053004 (2011), 1106.4359.

[47] I. K. Cooper, S. F. King, and C. Luhn (2012), 19 pages, 4 tables, 1203.1324.

[48] B.-Q. Ma (2012), 1205.0766.

[49] D. A. Eby and P. H. Frampton (2011), 1112.2675.

[50] X. Chu, M. Dhen, and T. Hambye, JHEP **1111**, 106 (2011), 1107.1589.

[51] H. Benaoum (2012), 1207.1967.

[52] S. Roy and N. N. Singh (2012), 1206.7016.

[53] I. de Medeiros Varzielas and L. Merlo, JHEP **1102**, 062 (2011), 1011.6662.

[54] T. Araki and C.-Q. Geng, JHEP **1109**, 139 (2011), 1108.3175.

[55] B. Brahmachari and A. Raychaudhuri (2012), 1204.5619.

[56] J. Liao, D. Marfatia, and K. Whisnant (2012), 1205.6860.

[57] S. Zhou (2012), 1205.0761.

[58] Z.-z. Xing (2012), 1205.6532.

[59] S. F. King and C. Luhn, JHEP **1109**, 042 (2011), 1107.5332.

[60] S. F. King and C. Luhn, JHEP **1203**, 036 (2012), 1112.1959.

[61] Y. Shimizu, M. Tanimoto, and A. Watanabe, Prog.Theor.Phys. **126**, 81 (2011), 1105.2929.

[62] E. Ma and D. Wegman, Phys.Rev.Lett. **107**, 061803 (2011), 1106.4269.

[63] Y. Ahn, S. Baek, and P. Gondolo (2012), 1207.1229.

[64] H. Ishimori and E. Ma (2012), 1205.0075.

[65] E. Ma, A. Natale, and A. Rashed (2012), 1206.1570.

[66] S. Antusch, S. F. King, C. Luhn, and M. Spinrath, Nucl.Phys. **B856**, 328 (2012), 13 pages, 2 figures/ version to appear in Nuclear Physics B, 1108.4278.

[67] S. F. King, JHEP **1101**, 115 (2011), 1011.6167.

[68] G. Branco, R. Felipe, F. Joaquim, and H. Serodio (2012), 1203.2646.

[69] B. D. Callen and R. R. Volkas (2012), 1205.3617.

[70] J. Heeck and W. Rodejohann, JHEP **1202**, 094 (2012), 1112.3628.

[71] S. F. King and C. Luhn, JHEP **0910**, 093 (2009), 0908.1897.

[72] P. Ferreira, W. Grimus, L. Lavoura, and P. Ludl (2012), 1206.7072.

[73] G.-J. Ding (2012), 42 pages, 2 figures, 1201.3279.

[74] S. F. King, C. Luhn, and A. J. Stuart, Nucl.Phys. **B867**, 203 (2013), 1207.5741.

[75] T. Araki and Y. Li (2011), 1112.5819.

[76] H. Ishimori and T. Kobayashi (2012), 1201.3429.

[77] S. Gupta, A. S. Joshipura, and K. M. Patel, Phys.Rev. **D85**, 031903 (2012), 1112.6113.

[78] H.-J. He and X.-J. Xu (2012), 1203.2908.

[79] R. de Adelhart Toorop, F. Feruglio, and C. Hagedorn, Nucl.Phys. **B858**, 437 (2012), 1112.1340.

[80] R. d. A. Toorop, F. Feruglio, and C. Hagedorn, Phys.Lett. **B703**, 447 (2011), 1+11 pages, 1 figure/ v2: matches journal version, 1107.3486.

[81] S.-F. Ge, D. A. Dicus, and W. W. Repko, Phys.Rev.Lett. **108**, 041801 (2012), accepted for publication in PRL, 1108.0964.

[82] A. Rashed (2011), 1111.3072.

[83] H.-J. He and F.-R. Yin, Phys.Rev. **D84**, 033009 (2011), 1104.2654.

[84] A. Aranda, C. Bonilla, and A. D. Rojas, Phys.Rev. **D85**, 036004 (2012), v1:24 pages, 4 figures,v2: references added,v3:25 pages, 4 figures, corrections and improvements have been made, all data and figures have been updated and typos fixed, 1110.1182.

[85] E. Lashin, M. Abbas, N. Chamoun, and S. Nasri (2012), 1206.4754.

[86] D. Meloni, JHEP **1110**, 010 (2011), 1107.0221.

[87] S. Zhou, Phys.Lett. **B704**, 291 (2011), 1106.4808.

[88] D. Meloni (2012), 1203.3126.

[89] S. Dev, R. R. Gautam, and L. Singh, Phys.Lett. **B708**, 284 (2012), 14 pages, 4 figures, 1 table, references added, 1201.3755.

[90] D. Meloni, S. Morisi, and E. Peinado (2012), 1203.2535.

[91] S. Morisi, K. M. Patel, and E. Peinado, Phys.Rev. **D84**, 053002 (2011), 1107.0696.

[92] K. Siyeon (2012), 1203.1593.

[93] Z.-Z. Xing, Chin.Phys. **C36**, 101 (2012), 1106.3244.

[94] H. Zhang and S. Zhou, Phys.Lett. **B704**, 296 (2011), 1107.1097.

[95] L. J. Hall, H. Murayama, and N. Weiner, Phys.Rev.Lett. **84**, 2572 (2000), hep-ph/9911341.

[96] N. Haba and H. Murayama, Phys.Rev. **D63**, 053010 (2001), hep-ph/0009174.

[97] A. de Gouvea and H. Murayama, Phys.Lett. **B573**, 94 (2003), hep-ph/0301050.

[98] A. de Gouvea and H. Murayama (2012), 1204.1249.

[99] J. Beringer et al. (Particle Data Group), Phys. Rev. **D86**, 010001 (2012).

[100] R. Nichol (2012), final MINOS Results, talk at Neutrinos 2012, neu2012.kek.jp.